Proceedings of IDETC/CIE 2006
ASME 2006 International Design Engineering Technical Conferences and
Computers and Information in Engineering Conference
September 10-13, 2006, Philadelphia, Pennsylvania, USA

DETC2006-99350

A KINEMATIC THEORY FOR PLANAR HOBERMAN AND OTHER NOVEL FOLDABLE MECHANISMS

Jiten Patel
Mechanical Engineering
Indian Institute of technology-Madras
Chennai 600036, India
pjiten@gmail.com

G. K. Ananthasuresh
Mechanical Engineering
Indian Institute of Science
Bangalore 560 012, India
suresh@mecheng.iisc.ernet.in

ABSTRACT
In this paper, we present a kinematic theory for Hoberman and other similar foldable linkages. By recognizing that the building blocks of such linkages can be modeled as planar linkages, different classes of possible solutions are systematically obtained including some novel arrangements. Criteria for foldability are arrived by analyzing the algebraic locus of the coupler curve of a PRRP linkage. They help explain generalized Hoberman and other mechanisms reported in the literature. New properties of such mechanisms including the extent of foldability, shape-preservation of the inner and outer profiles, multi-segmented assemblies and heterogeneous circumferential arrangements are derived. The design equations derived here make the conception of even complex planar radially foldable mechanisms systematic and easy. Representative examples are presented to illustrate the usage of the design equations and the kinematic theory.

INTRODUCTION
This paper is concerned with foldable linkages. The applications of such linkages range from consumer products and toys to architectural applications and massive deployable space structures. They belong to the class of over-constrained linkages. It is their particular arrangement of specially designed, suitably-proportioned rigid links that renders them mobile often with a single degree of freedom. Therefore we see such mechanisms as inventions rather than results of systematic design. Two such examples are shown in Figs.1 and 2 [1]. In Fig. 1, we see the Hoberman's sphere—a popular toy in recent times [2]. Its planar version is shown in Fig. 2. Now, consider a general arrangement shown in Fig. 3. This paper poses the question: what geometry of links makes this over-constrained planar arrangement fold like Hoberman's mechanism of Fig. 2? Is Hoberman's the only possible solution? If not, how do we find the others? This paper answers these questions by deriving kinematic design equations that not only help explain this but also lead to general classes of foldable linkages.

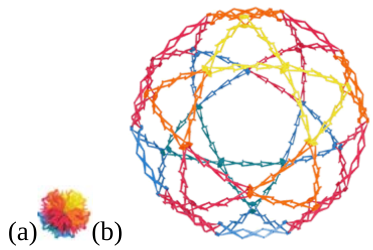

Figure 1. Hoberman's radially foldable sphere (a) folded (b) unfolded (images are approximately to the same scale.)

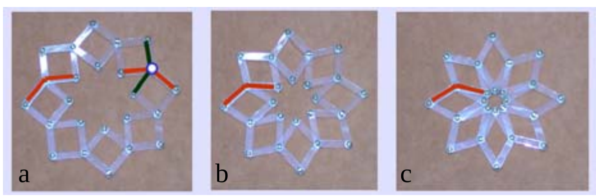

Figure 2. Hoberman's planar foldable mechanism. The basic building block is shown using superimposed red angulated line in (a-c). Figure (a) also highlights the basic pair that folds.

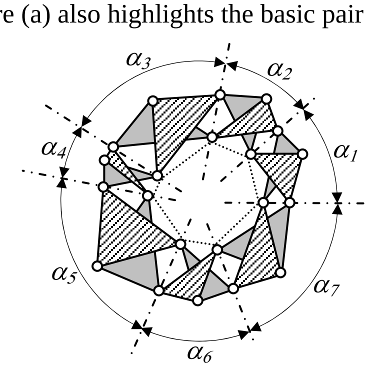

Figure 3. An arbitrary closed loop of a potentially foldable linkage.

According to You and Pellegrino [3], there are two types of foldable structures. Some are specific in that their arrangement of bars and revolute joints gives their specific foldability while others consist of repeating building blocks that can lead to a variety of foldable designs. In the latter type, a remarkable invention of a patented angulated bar element by Hoberman [1] has proved to be versatile in giving a wide range of 2-D and 3-D foldable structures with a single degree of freedom. Indeed the basic building block of the mechanism in Fig. 2 is a bent bar with an obtuse angle as shown by thick angulated lines in all three Figs. 2(a-c). In this structure there are 16 angulated elements connected with 24 hinges. In Fig. 2a, a hinge between two adjacent elements is shown. According to the Grubler's formula, it has 3(16-1) – 2(24) = -3 degrees of freedom. But, how did Hoberman arrive at the above arrangement and the lengths and the angle of his building block so that it can fold with a single degree of freedom? Is this the only radially foldable mechanism? The answer is 'no' because You and Pellegrino [3] have reported their inventions of two types of generalized angulated elements (GAEs). They give many examples of not only circular but also general shapes that can fold in this manner. They also propose a multi-angulated element to minimize the number of elements in a complex arrangement. They present a number of designs and geometric derivations. In this paper, based on a simple kinematic interpretation we derive general conditions of foldability and establish a class of solutions which render Hoberman's and You and Pellegrino's designs as special classes and cases. Furthermore, we also present conditions for shape-preservation of the interior inscribed polygon (shown with a dotted line in Fig. 3).

Since the focus of this paper is on kinematic analysis of foldable structures, it is pertinent to note that kinematic treatment of foldable linkages is receiving increasing attention in recent years. Wohlhart [4] reported a number of three dimensional foldable linkages. Langbecker [5] presented kinematic analysis of scissor structures and derived the foldability conditions. The basic element of a scissor structure is a pair of straight bars connected with a revolute joint to form an X (scissor) shape. Lazy tongs is an example of such a structure. Langbecker also considered Hoberman's angulated element but not the more general ones discovered by You and Pellegrino [3]. Dai and Jones [6] analyzed the mobility of foldable mechanisms which belong to a general class of metamorphic mechanisms. They used principles of screw theory to arrive at mobility conditions [7]. Agrawal et al. [8] presented a design methodology for constructing foldable linkages of general shapes. Langbecker and Albermani [9] discussed the geometric design of foldable structures of positive and negative curvatures and also analyzed the structural response of such structures. Pfister and Agrawal [10] considered the dynamics of suspended foldable structures. While the above works used analytical tools such as screw theory and Euler-Liouville equations or plain trigonometry, the present work uses the classical theory of algebraic equations of loci of points in a linkage. This simple theory surprisingly leads to many more insights into the kinematics of planar foldable linkages and leads to general classes of solutions and straightforward design criteria.

In the next section, our recent work [11] on kinematic interpretation of radially foldable mechanisms and the equation of a coupler curve are briefly reviewed. This paper utilizes and adds to it to derive the conditions of foldability and shape-preservation and other new kinematic insights including the extent of foldability, heterogeneous arrangements of basic pairs of angulated elements, multi-segmented assemblies, etc. Some concluding remarks are in order at the end of the paper.

KINEMATIC INTERPRETATION OF HOBERMAN TYPE FOLDABLE LINKAGES

Figure 4a shows a pair of Hoberman's angulated elements that enclose an angle α at the center. Since points *A*, *C*, *D* and *E* are constrained to move along the dashed lines, we can interpret the angulated elements as PRRP linkages. Figure 4b shows this for the angulated element *ABC*. It should be observed that in the Hoberman's element, point *B*, which we can call the coupler point of the PRRP linkage, traces a radial line indicated as a dotted line in Fig. 4b. If we take a general pair of angulated elements (or as a pair of general PRRP linkages) as in Fig. 4c, we can easily see that Grubler's formula gives zero degrees of freedom. Thus, this pair is immovable in general. But its mobility is essential for the foldability of the polar array of such a pair. By noting that two PPRP linkages are individually movable with a single degree of freedom, we can say that the two pair will be movable if they both share the same coupler curve at point *B*. *This is a simple but effective condition as can be seen when the equation of the coupler curve is derived.*

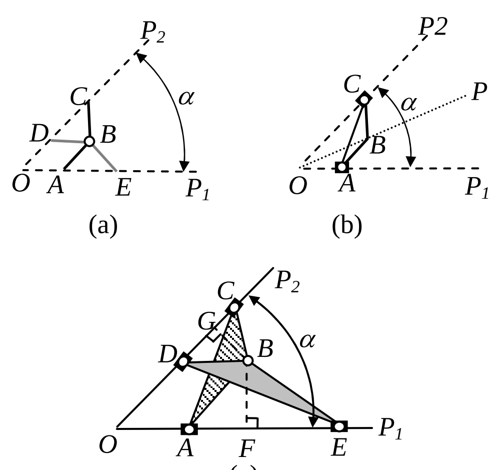

Figure 4. Kinematic interpretation of Hoberman's angulated element (a) a pair of Hoberman's angulated elements (b) a PRRP linkage interpretation of an angulated element (c) a pair of general PRRP linkages sharing a common coupler point *B*.

Equation of the coupler curve of a PRRP linkage

The equation of the coupler curve of a 4R four-bar linkage is a special sextic with many interesting properties [12]. There have been attempts to synthesize path-generating four-bar linkages using its equation [e.g., 13, 14]. Using the same procedure as in [12], the algebraic equation of the coupler curve of the PRRP linkage is derived below.

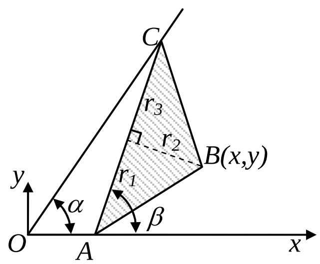

Figure 5. A PRRP linkage and its coupler point

From the symbols defined in Fig. 5 and letting the coordinates of the coupler point *B* be (x, y), the coordinates of points *A* and *C* can be written as follows:

$$\begin{aligned} &A: (x - r_1\cos\beta - r_2\sin\beta,\ y - r_1\sin\beta + r_2\cos\beta) \\ &C: (x + r_3\cos\beta - r_2\sin\beta,\ y + r_3\sin\beta + r_2\cos\beta) \end{aligned} \tag{1}$$

Since *A* lies on the x-axis and *C* on the line given by $y = (\tan\alpha)\ x$, we can write

$$\begin{aligned} &y_A = y - r_1\sin\beta + r_2\cos\beta = 0 \\ &y + r_3\sin\beta + r_2\cos\beta = \tan\alpha\left(x + r_3\cos\beta - r_2\sin\beta\right) \end{aligned} \tag{2}$$

By solving for $\cos\beta$ and $\sin\beta$ using the two equations in Eq. (2), and using the identity $\sin^2\beta + \cos^2\beta = 1$, the equation of the coupler can be obtained. It has the following form.

$$\begin{aligned} &(r_1^2\tan^2\alpha + r_2^2\tan^2\alpha)x^2 + (r_2^2\tan^2\alpha + r_3^2\tan^2\alpha \\ &+2r_1r_2\tan\alpha + 2\ r_2r_3\tan\alpha + r_1^2 + r_3^2 + 2r_1r_3)\ y^2 \\ &+2(-r_1r_2\tan^2\alpha - r_2r_3\tan^2\alpha - \ r_1^2\tan\alpha - r_1r_3\tan\alpha)\ xy + \\ &(-2r_2^3r_3\tan\alpha - r_2^2r_1^2 - r_3^2r_1^2\tan^2\alpha - 2r_1r_2^3\tan\alpha - 2r_1r_2^2r_3 \\ &-r_2^4\tan^2\alpha - r_2^2r_3^2 + 2r_1r_2r_3^2\tan\alpha + 2r_1^2r_2r_3\tan\alpha + 2r_1r_2^2r_3\tan^2\alpha) \end{aligned} \tag{3}$$

Compared to the full form of a 2nd degree equation, which is shown below, Eq. (3) has a shortened form with $g = f = 0$.

$$ax^2 + by^2 + 2hxy + 2gx + 2fy + c = 0 \tag{4}$$

For different parameters, $\{r_1, r_2, r_3, \alpha\}$, of the PRRP linkage, the coupler curve will trace different geometric entities as summarized below.

$$\begin{aligned} &\text{(i) A pair of straight lines if} \\ &\quad \Delta = abc + 2fgh - af^2 - bg^2 - ch^2 = abc - ch^2 = 0. \\ &\text{(ii) A parabola if } h^2 - ab = 0 \text{ and } \Delta \neq 0. \\ &\text{(iii) A hyperbola if } h^2 - ab > 0 \text{ and } \Delta \neq 0. \\ &\text{(iv) An ellipse if } h^2 - ab < 0 \text{ and } \Delta \neq 0. \\ &\text{(v) A pair of parallel lines if } h^2 - ab = 0 \text{ and } \Delta = 0 \end{aligned} \tag{5}$$

Condition for the Hoberman's mechanism

To obtain the condition on the parameters $\{r_1, r_2, r_3, \alpha\}$ to give the Hoberman's mechanism, we note that in his mechanism all the coupler points trace radial lines passing through the center. Therefore, we can apply condition (i) of Eq. (5) and arrive at the following relationship.

$$\tan\alpha = \frac{r_2(r_1 + r_3)}{r_1r_3 - r_2^2} \tag{6}$$

It is a special situation of identical straight lines passing through the origin both having the form $y = mx$.

We note that the condition of Eq. (6) is more general than a Hoberman element. We need to reduce this equation further to make it specific to a Hoberman's angulated element. We note that even in the general type, Hoberman assumes that the two triangles (or the angulated bars) in the pair are identical. A special case, which is shown in Figs. 2a-c, is obtained when the two sides enclosing the obtuse angle are equal. That is, $r_1 = r_3$. This relationship with Eq. (6) would give the result that $\angle BOA = \angle BCA = \angle BAC = \alpha/2$ in Fig. 5.

$$\begin{aligned} &\tan\alpha = \frac{r_2(r_1 + r_3)}{r_1r_3 - r_2^2} = \frac{2r_2r_1}{r_1^2 - r_2^2} = \frac{2(r_2/r_1)}{1 - (r_2/r_1)^2} \\ &\Rightarrow \tan(2\cdot\alpha/2) = \frac{2\tan(\tan^{-1}(r_2/r_1))}{1 - \tan^2(\tan^{-1}(r_2/r))} \end{aligned} \tag{7}$$

with $\tan(\alpha/2) = r_2/r_1$

Thus, Hoberman's mechanism of Figs. 2a-c is easily seen as a special case of designs governed by Eq. (6). In fact, the coupler curve interpretation and this equation for radial coupler curve lead to many insights into the planar radially foldable linkages of this kind. These are discussed next.

PROPERTIES OF RADIALLY FOLDABLE LINKAGES

By referring to Fig. 3 once again, now with the help of the above kinematic interpretation and the equation of the coupler curve, we can derive the conditions for foldability and shape-preservation. By 'foldability', we mean that such a linkage will have a positive number of kinematic degrees of freedom. We prefer it to be one in practice. By 'shape-preservation' we mean that the shape of the inscribed polygon in Fig. 3 retains its shape as the linkage folds radially inwards or outwards. For the example shown in Fig. 2, this inscribed polygon is a regular octagon that preserves its shape during folding.

Foldability condition

From Fig. 4c, it is to be noted that the pair of PRRP linkages will have one degree of freedom when they both share the same coupler curve at their common point *B*. Now, if take two arbitrary instances of the parameters $\{r_1, r_2, r_3\}$ for the same α, what relationship among them gives rise to the same equation of the coupler curve? One possible solution to this is a generalized angulated element of the first kind (GAE1) given by You and Pellegrino, which they call an invention. In GAE1, as shown in Fig. 6, there is a simple condition of isosceles triangle that relate the two instances of $\{r_1, r_2, r_3\}$.

As shown in Fig. 6, a pair of PRRP linkages is considered. Note that we have used the parameters $\{r_1, r_2, r_3, \alpha\}$ for one linkage and $\{s_1, s_2, s_3, \alpha\}$ for another. You and Pellegrino define GAE 1 as the one in which the triangles ABE and DBC are isosceles such that $AB = EB$ and $DB = CB$, i.e.,

$$\sqrt{r_1^2 + r_2^2} = \sqrt{s_1^2 + s_2^2} \text{ and } \sqrt{r_2^2 + r_3^2} = \sqrt{s_2^2 + s_3^2}\ . \tag{8}$$

We show below that this condition can easily be verified by using the equation of the coupler curve. We do this by showing that the coupler curves of both the PRRP linkages are the same when the above isosceles triangle condition is satisfied by the parameters $\{r_1, r_2, r_3, \alpha\}$ and $\{s_1, s_2, s_3, \alpha\}$.

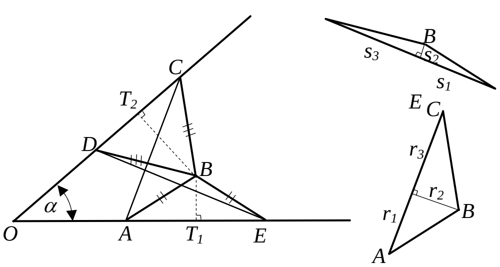

Figure 6. The case of isosceles triangles (GAE 1) of [3]

Perpendiculars BT_1 and BT_2 are drawn so that OT_1BT_2 becomes a cyclic quadrilateral so that

$$\begin{aligned}
&\alpha + \angle T_1BT_2 = \pi \\
&\alpha + \angle T_1BA + \angle ABD + \angle DBT_2 = \pi \\
&\Rightarrow \alpha + \frac{\angle DBE - \angle ABD}{2} + \angle ABD + \frac{\angle ABC - \angle ABD}{2} = \pi \\
&\Rightarrow \angle DBE + \angle ABC = 2(\pi - \alpha)
\end{aligned} \tag{9}$$

Since angles $\angle ABC$ and $\angle DBE$ are in terms of the parameters $\{r_1, r_2, r_3, \alpha\}$ and $\{s_1, s_2, s_3, \alpha\}$, we can substitute Eqs. (8) and (9) into the equation of the coupler curves defined by $\{r_1, r_2, r_3, \alpha\}$ and $\{s_1, s_2, s_3, \alpha\}$ to see that they are the same in view of Eq. (8). It is important to note that under the isosceles triangles condition, the coupler curve shared by the two PRRP linkages is an ellipse.

A second possibility of having the same coupler curve for two instances of $\{r_1, r_2, r_3\}$ is that the coupler curve is a radial line passing through the center. The condition for it is already given in Eq. (6). The generality of this equation can be highlighted by the fact that it gives You and Pellegrino's [3] another invention called the generalized angulated element of the second kind (GAE2).

GAE 2 is defined as a pair of PRRP linkages in which triangles ΔABE and ΔDBC are similar. This geometric condition observed by You and Pellegrino to give foldability indeed gives radial-line for the common coupler point. To show that Eq. (6) readily gives this condition, we state and prove two propositions: (i) When ΔABE and ΔDBC are similar it leads to Eq. (6), and (ii) When Eq. (6) is satisfied, ΔABE and ΔDBC are similar.

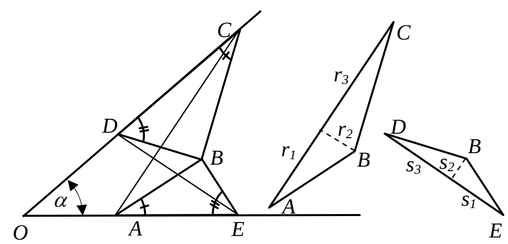

Figure 7. The case of similar triangles (GAE 2) of [3]

Proof of proposition 1: By referring to Fig. 7, due to the similarity of ΔABE and ΔDBC, we can write

$$\text{(i) } \angle AEB = \angle CDB \text{ and (ii) } \angle EAB = \angle DCB \tag{10}$$

By noting that

$$\begin{aligned}
&\angle AEB = \angle AED + \tan^{-1}(s_2 / s_1) = \angle OED + \tan^{-1}(s_2 / s_1) \\
&\angle CDB = \pi - \tan^{-1}(s_2 / s_3) - \angle ODE = \\
&\pi - \tan^{-1}(s_2 / s_3) - (\pi - \alpha - \angle OED)
\end{aligned} \tag{11}$$

from (i) of Eq. (10), we get

$$\begin{aligned}
&\angle OED + \tan^{-1}(s_2 / s_1) = \pi - \tan^{-1}(s_2 / s_3) - (\pi - \alpha - \angle OED) \\
&\Rightarrow \alpha = \tan^{-1}(s_2 / s_1) + \tan^{-1}(s_2 / s_3) = \tan^{-1}\left(\frac{s_2(s_1 + s_3)}{s_1 s_3 - s_2^2}\right) \\
&\Rightarrow \tan\alpha = \frac{s_2(s_1 + s_3)}{s_1 s_3 - s_2^2}
\end{aligned} \tag{12}$$

Similarly, from (ii) of Eq. (10), we can see that

$$\Rightarrow \tan\alpha = \frac{r_2(r_1+r_3)}{r_1 r_3 - r_2^2} \tag{13}$$

Eqs. (12) and (13) are the same as Eq. (6). QED.

Proof of proposition 2 (converse of proposition 1):
Now, we have

$$\tan\alpha = \frac{s_2(s_1+s_3)}{s_1 s_3 - s_2^2} \text{ and } \tan\alpha = \frac{r_2(r_1+r_3)}{r_1 r_3 - r_2^2}. \tag{14}$$

We take the first one of Eq. (14) and divide the numerator and the denominator of the right hand side by $s_1 s_3$ to get

$$\begin{aligned} \tan\alpha &= \frac{(s_2/s_1)+(s_2/s_3)}{1-(s_2/s_1)(s_2/s_3)} \\ \Rightarrow \alpha &= \tan^{-1}\left(\frac{(s_2/s_1)+(s_2/s_3)}{1-(s_2/s_1)(s_2/s_3)}\right) \\ &= \tan^{-1}(s_2/s_1)+\tan^{-1}(s_2/s_3) \end{aligned} \tag{15}$$

which is part of Eq. (12) and can be arranged to give the result that $\angle ABE = \angle CDB$. Similar procedure for the second part of Eq. (14) gives $\angle EAB = \angle DCB$. This leads to the conclusion that ΔABE and ΔDBC are similar. QED.

One of the numerous linkages designed with Eq. (6) is shown in Fig. 8 in eight different configurations. Thus, this equation not only helps in systematically deriving inventions reported by Hoberman [1] and You and Pellegrino [3] but also helps in constructing new designs. Since, we now understand the conditions for foldability, we can easily construct heterogeneous designs where non-identical pairs of PRRP linkages are connected together to form of foldable closed-loop linkages. Two examples of this are shown in Figs. 9 and 10. While Fig. 9 has a regular pattern with two different pairs of PRRP linkages, Fig. 10 has completely different pairs used to create the closed loop. Two things can be observed in the linkage of Fig. 10. First, the shape of its inscribed polygon (see Fig. 3) is not preserved. Second, it is not capable of folding completely. Both of these properties can be discerned from the equation of the coupler curve with further analysis.

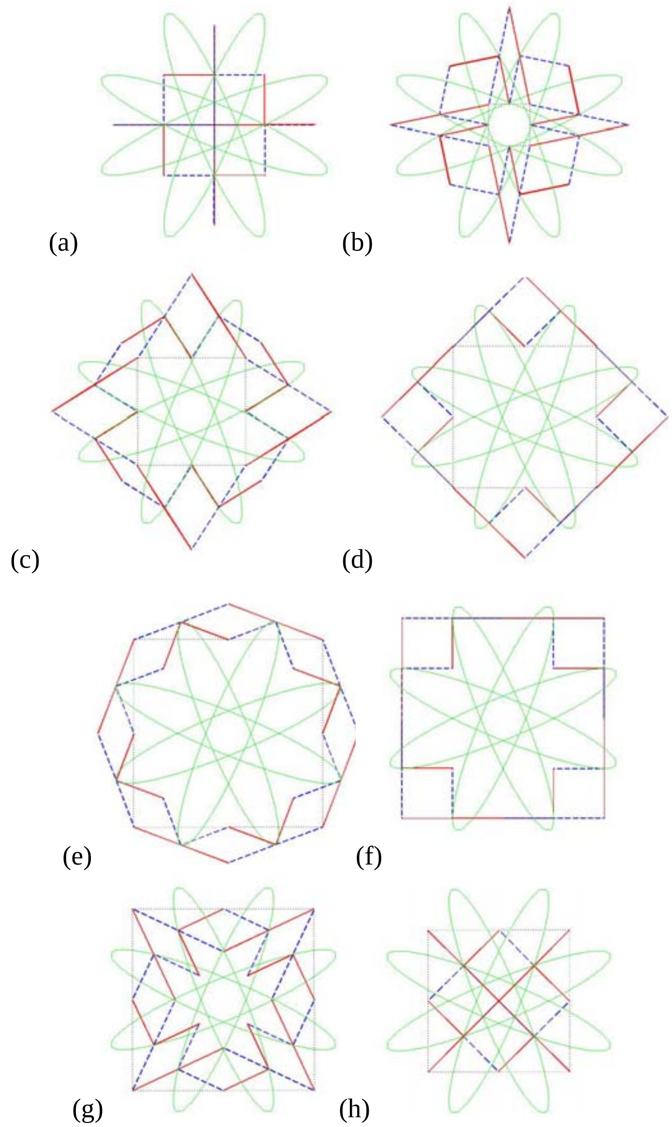

Figure 8. Eight configurations of a fully and reversibly foldable linkage, one of the many possible linkages that can be designed with Eq. (6). Elliptical loci of the coupler points are also shown.

Partial foldability of heterogeneous arrangements

Hoberman's angulated element pairs are identical and hence they are foldable completely. But when two non-identical PRRP linkages are connected together at a common coupler point, they may not in general be foldable completely. This means that when a circumferentially closed linkage consisting of several such heterogeneous pairs, the inscribed polygon will not be able to shrink to a point. So, one needs to analyze the extent and the range of foldability. This can be analyzed once again with the help of the equation of the coupler curve and insights gained from it.

Consider the PRRP linkage shown in Fig. 11 and let its parameters $\{r_1, r_2, r_3, \alpha\}$ satisfy the radial-line coupler point condition of Eq. (6). Let the size of this linkage be fixed so that $r_1 + r_3 = 1$. Then, for a given α and r_1/r_3, r_2 will be determined by Eq. (6). This implies that there is a freedom to choose the coupler point B by choosing the value of r_1/r_3.

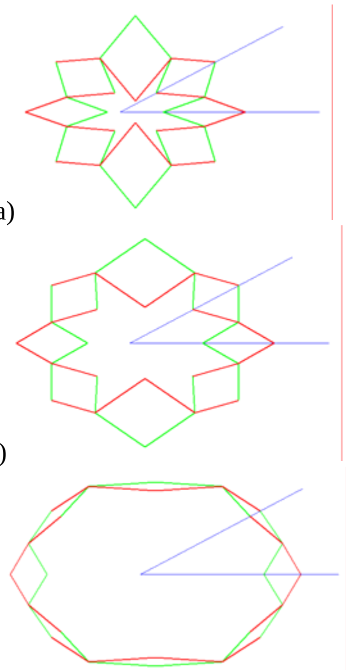

(a)

(b)

(c)

Figure 9. Three configurations of a heterogeneous regular foldable linkage. The inscribed polygon of this is a rectangle with rounded corners.

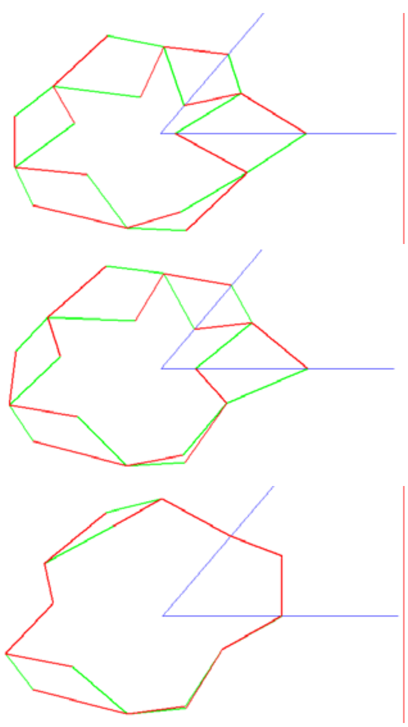

(a)

(b)

(c)

Figure 10. Three configurations of a heterogeneous irregular radially foldable linkage. The inscribed polygon does not retain its shape here.

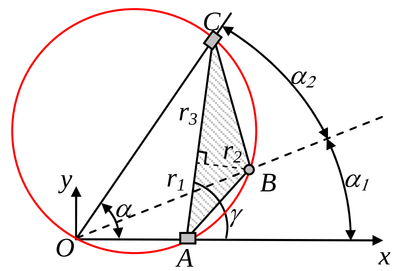

Figure 11. Possible locations of the coupler point to have a radial line as its locus.

It can be shown that *B* can lie anywhere on the (red) circle shown in Fig. 11. All these coupler points will have radial line as their locus as the PRRP linkage moves. This leads to an interesting consequence: OABC is a cyclic quadrilateral. Therefore, the following angles in the same segment of the circle are equal.

$$\begin{aligned} \angle AOB &= \angle ACB = \alpha_1 \\ \angle BOC &= \angle BAC = \alpha_2 \end{aligned} \tag{16}$$

From Fig. 11, we can also see that

$$\angle ABC = \pi - (\alpha_1 + \alpha_2) = \pi - \alpha \tag{17}$$

Using these relationships, we can also derive the radius of the circle in Fig. 11 to be equal to $(2\sin\alpha)^{-1}$ for the size-normalization condition of $r_1 + r_3 = 1$. Based on this, we can derive the analytical expressions for the lengths $\overline{OA}$, $\overline{OB}$ and $\overline{OC}$ from the coordinates of points *A*, *B*, and *C*.

$$\begin{aligned} &A:\{a = \sin(\gamma-\alpha)/\sin\alpha, 0\} \\ &B:\{a + r_1\cos\gamma + r_2\sin\gamma, r_1\sin\gamma - r_2\cos\gamma\} \\ &C:\{a + \cos\gamma, \sin\gamma\} \end{aligned} \tag{18}$$

In Eq. (18), γ is the variable that exercises the single degree of freedom of the PRRP linkage. In view of investigating the extent of foldability, we restrict the range of γ to $\alpha \le \gamma \le \pi$. With reference to Fig. 12, where the length $\overline{OB}$ is plotted for three different values of r_1/r_3. A heterogeneous PRRP linkage pair can be made if there are two values of γ for a given value of $\overline{OB} = b$. This is because the two linkages share a common coupler point as seen in Fig. 4c. Among the three cases shown in Fig. 12, only $r_1/r_3 = 1$ shows full foldability because of the symmetric nature of the curve in the permitted range of γ. The reduced ranges of foldability for the other two cases are also shown in the figure. Thus, partial foldability can be analytically characterized.

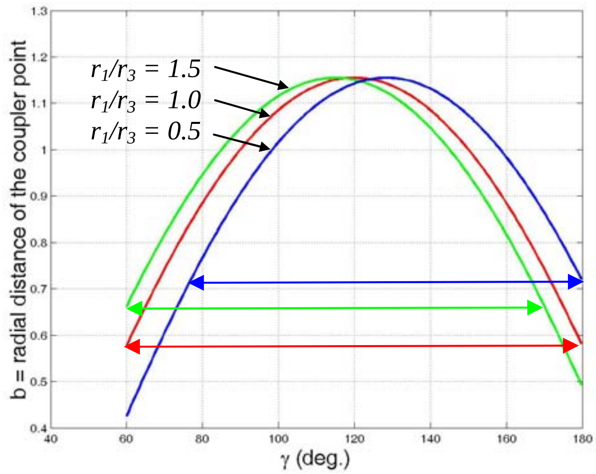

Figure 12. Extent of foldability of heterogeneous PRRP linkage pairs.

Multi-segment assemblies

You and Pellegrino [3] note that the angulated element need not contain only two segments and can consist of any number of segments of equal length. But they limit it to the case where all segments are of equal length. The radially foldable multi-segment mechanism created using You and Pellegrino's idea is shown in Figure 13. Based on the result indicated in Figs. 11 and 14, we note that an entire arc (actually the circle as a whole) can be used for this purpose as all the points on it trace radial lines. As shown in Fig. 14, this circle rotates about the origin as the PRRP linkage moves. Its locus is shown in the last figure of Fig. 14.

Figure 13. A multi-segmented assembly of a radially foldable planar linkage.

Shape-preservation

You and Pellegrino [3] presented some foldable linkages where the inscribed polygon (see Fig. 3) can assume a variety of shapes. But not all of them preserve that shape as the mechanism moves with a single degree of freedom. No conclusive conditions for shape-preservation were given in that work. Having derived the analytical expressions for $\overline{OA}$ and $\overline{OC}$, it is now a simple matter to see when the shape will be preserved: the velocities of points *A* and *C'* (where *A* belongs to one PRRP linkage and *C'* to the other in the pair) should be proportional to their distances from the origin. If the parameters of the linkage satisfy this condition, we can ensure shape-preservation for any arbitrary circumferentially closed-loop linkage such as the one shown in Fig. 3. If it is not possible, it will be revealed as well.

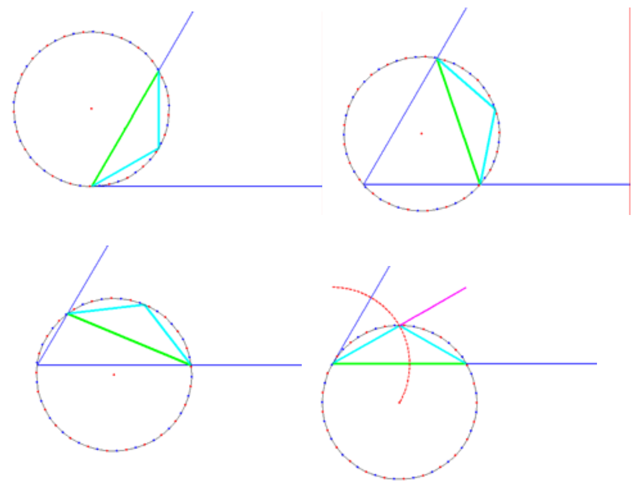

Figure 14. Possible radial-line coupler point locus to create multi-segment assemblies. All the points on the circle trace radial lines.

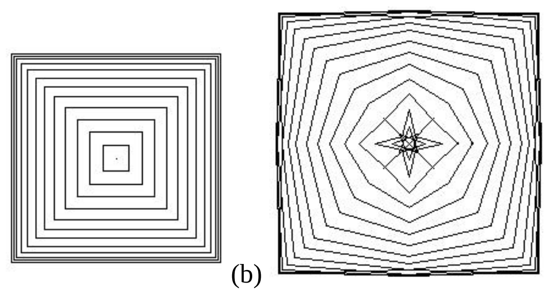

(a) (b)

Figure 15. Interior polygon shapes of the linkage shown in Fig. 8. (a) Shape-preserving case (b) shape-changing case

Figures 15a-b show the cases of interior polygon with preserved shape and change shape. Fig. 15a corresponds to the case of the linkage shown in Fig. 8. Fig. 15b is an asymmetric variation of it with changing shape. Figure 17a-b show the case of a closed-loop linkage with seven building blocks, i.e., seven PRRP linkages. In this case, since r_1/r_3 is equal to one, we have the shape of the polygon preserved. On the other hand, in Fig. 17c-d, r_1/r_3 is less than one and the shape is not preserved. It is interesting to see that now, the linkage is not closed and the points on the x-axis need to be guided along the x-axis. It also gives an interesting possibility that changing the distance between the un-joined points on the x-axis provides an easy way to actuate this single degree-of-freedom linkage.

Figure 18 shows the prototype of a heterogeneous linkage, which has the interior polygon of the shape of a pentacle. Finally, Fig. 19 shows a compliant one-piece linkage that is foldable and is designed based on the design equations presented in the paper. Details of this design are presented elsewhere.

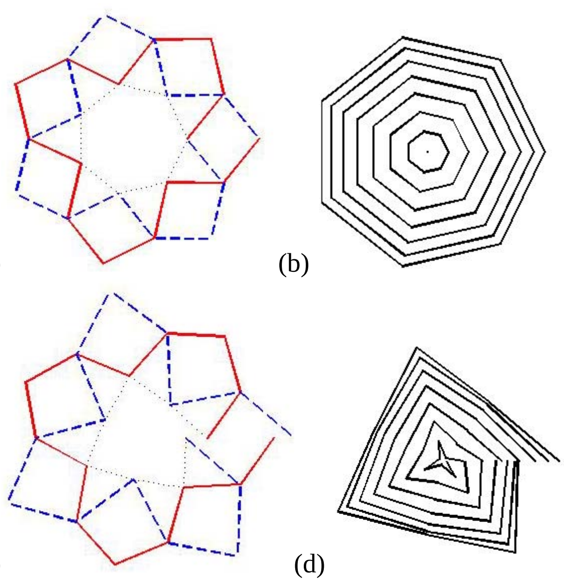

(a) (b) (c) (d)

Figure 17. (a-b) A seven-module foldable linkage and its shape-preserving regular heptagons (c-d) An open heterogeneous linkage whose points on the horizontal need to be guided, and its shape-changing interior polygon. The guided points can easily be actuated with a linear actuator. Thus, even an irregular shape can be closed and opened with this type of linkages.

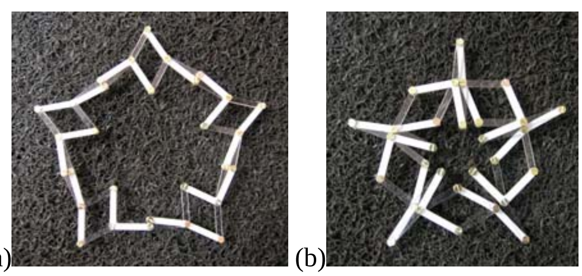

(a) (b)

Figure 18. A heterogeneous foldable linkage prototype made using polypropylene (white) and Plexiglas (transparent) materials to show the two different building blocks.

(a) (b) (c)

Figure 19. A foldable compliant, single-piece linkage design using the design equations presented in this paper.

CLOSURE

In this paper, we presented the kinematic theory behind Hoberman's and other inventions related to planar, radially foldable linkages. Apart from rigorously explaining why overconstrained linkages such as Hoberman's structures have mobility, we showed that a general class of foldable linkages can be derived by using a simple algebraic equation and even simpler design criterion. This criterion was derived from the kinematic interpretation that the basic building block in the radially foldable linkages is a pair of PRRP linkages. The algebraic equation of the locus of the coupler point of the PRRP linkage reveals the reported inventions as special cases. It also helps in providing further design insights into several interesting properties such as foldability, shape-preservation, heterogeneous arrangements, multi-segment assemblies, circumferential actuation, etc. Future extensions of this work inclide 3-D radially foldable linkages, giving a suitable shape to the angulated elements to ensure complete coverage, etc. Applications of the theory presented here to deployable linkages/structures for architectural and space requirements is currently being pursued in our ongoing work.

ACKNOWLEDGMENTS

This work was an outgrowth of a project funded by the BRNS program of the Government of India in which a compliant foldable mechanism is being designed. This support is gratefully acknowledged. The authors thank Pradeep Biradar for his help in fabricating the prototypes whose pictures are include in this paper.

REFERENCES

1. Hoberman. C, 1991, "Radial Expansion/Retraction Truss Structures," *US patent* 5,024,031.
2. http://www.hoberman.com
3. You, Z. and Pellegrino, S.,"Foldable Bar Structures," *Intl. Journal of Solids and Structures*, 34 (1996), pp. 1825-1847.
4. Wohlhart, K., "New Overconstrained Spheroidal Linkages," World Congress on the Theory of Machines and Mechanisms, Milano, Italy, 1995, Vol. 1, pp. 149-154.
5. Langbecker, T., 1999, "Kinematic Analysis of Deployable Scissor Structures," International Journal of Space Structures, Vol. 14, No. 1, pp. 1-15.
6. Dai, J.S. and Rees Jones, J., Mobility in Metamorphic Mechanisms of Foldable/Erectable Kinds, Journal of Mechanical Design, Transaction of ASME, vol 121(3), 1999, pp. 375-382.
7. Agrawal, S. K., Kumar, S. and Yim, M., "Polyhedral Single Degree-of-freedom Expanding Structures: Design and Prototypes," Journal of Mechanical Design, Vol. 124, 2002, pp. 473-478.
8. Dai, J.S., Li, D., Zhang, Q. and Jin, G.G., Mobility Analysis of a Complex Structured Ball Based on Mechanism Decomposition and Equivalent Screw System Analysis, Mechanism and Machine Theory, Vol. 39, pp. 445-458, 2004.

9. Langbecker, T. and Albermani, F., “Foldable Positive and Negtaive Curvature Structures: Geometric Design and Structural Response,” Journal of the International Association for Shell and Spatial Structures, Vol. 41, No. 3, 2000, pp. 147-169.
10. Pfister, F. M. J. and Agrawal, S. K., “Analytical Dynamics of Unrooted Multibody Systems with Symmetries,” Journal of Mechanical Design, Vol. 121, 1999, pp. 440-447.
11. Patel, J. and Ananthasuresh, G. K., “Kinematics of Radially Foldable Mechanisms using Algebraic Loci,” Proceedings of the 3rd Aerospace and Related Mechanisms (ARMS 2005) Conference of INSARM (Indian Society of Aerospace and Related Mechanisms), Bangalore, India, Nov. 16-19, 2005.
12. Hunt, K. H., *Kinematic Geometry of Mechanism*s, Oxford University Press, 1978.
13. Blechschimdt, J. L. and Uicker, J. J., “Linkage Synthesis Using Algebraic Curves,” Journal of Mechanisms, Transmissions, and Automation in Design, Vol. 108, 1986, pp. 543-548.
14. Ananthasuresh, G.K. and Kota, S., “A Renewed Approach to the Synthesis of Four-bar Linkages for Path Generation via the Coupler Curve Equation,” Proceedings of the *National Applied Mechanisms and Robotics Conference*, Paper 83, Cincinnati, OH, Nov. 8-10, 1993.